JOURNAL OF MOLECULAR SPECTROSCOPY 106, 280–298 (1984)

Molecular Beam Electric Resonance Study of KCN, $K^{13}CN$ and $KC^{15}N$

J. J. VAN VAALS,[1] W. LEO MEERTS, AND A. DYMANUS

Fysisch Laboratorium, Katholieke Universiteit, Toernooiveld, 6525 ED Nijmegen, The Netherlands

The microwave spectra of the isotopic species $K^{13}CN$ and $KC^{15}N$ have been investigated by molecular beam electric resonance spectroscopy, using the seeded beam technique. For both isotopic species about 20 rotational transitions originating in the ground vibrational state were observed in the frequency range 9–38 GHz. The observed transitions were fitted to an asymmetric rotor model to determine the three rotational, as well as the five quartic and three sextic centrifugal distortion constants. The hyperfine spectrum of KCN has been unravelled with the help of microwave–microwave double-resonance techniques. One hundred and forty hyperfine transitions in 11 rotational transitions have been assigned. The hyperfine structures of $K^{13}CN$ and $KC^{15}N$ were also studied. For all three isotopic species the quadrupole coupling constants and some spin–rotation coupling constants could be deduced. The rotational constants of the ^{13}C and ^{15}N isotopically substituted species of potassium cyanide, combined with those of the normal isotopic species (determined more accurately in this work), allowed an accurate and unambiguous evaluation of the structure, which was confirmed to be T shaped. Both the effective structure of the ground vibrational state and the substitution structure were evaluated. The results for the effective structural parameters are r_{CN} = 1.169(3) Å, r_{KC} = 2.716(9) Å, and r_{KN} = 2.549(9) Å. The values obtained for the principal hyperfine coupling constant eQq_z(N), the angle between the CN axis and z_N, and the bond length r_{CN} indicate that in gaseous potassium cyanide the CN group can be considered as an almost unperturbed CN^- ion.

1. INTRODUCTION

Gaseous alkali metal cyanides[2] are floppy molecules. They possess large zero-point bending motion amplitudes (*1–3*) of up to 15°. The potential energy barrier in the bending direction is small (less than 0.3 eV) (*1–4*), and vibrational excitation can change the structure of the molecule drastically. At high temperatures it will even be possible for the M^+ cation to orbit around the CN^- anion. Since no unique structure can be assigned in this case, Clementi *et al.* (*4*) named this type of bonding for LiNC "polytopic." The Born–Oppenheimer approximation breaks down since the motions of electrons and nuclei are strongly coupled, and the rovibrational spectrum of the molecule cannot be described with a (semi)rigid rotor or small-amplitude vibrator model. Studies of the alkali metal cyanides give a more complete understanding of molecules with weak internal interaction.

[1] Present address: Philips Research Laboratories, 5600 MD Eindhoven, The Netherlands

[2] In this paper the alkali metal cyanides are denoted by MCN (where M represents the alkali metal), whatever the structure may be, and the atomic symbol designates the most abundant isotope, unless specified otherwise.

0022-2852/84 $3.00

Until recently, the structure of the KCN, NaCN, and LiNC molecules was assumed to be linear. For KCN, a linear cyanide configuration was deduced by Ismail *et al.* (*5*) from vibrational isotope effects of potassium cyanide in inert gas matrices, and by Pietro *et al.* (*6*) from *ab initio* calculations. Kuijpers *et al.* (*7*) reported the first successful observation of the microwave absorption spectrum of KCN between 85 and 107 GHz. It was, however, not possible to determine the structure, since a tentative fit of some observed lines to a linear rotor model resulted in improbable structural parameters. A correct identification was impeded by the appearance of at least 11 vibrational states in the observed rotational spectrum. However, microwave absorption experiments at Berlin and molecular beam electric resonance experiments at Nijmegen established that the most stable structure of KCN in the ground vibrational state is T shaped (*8, 9*). Since only one, the most abundant, isotopic species was measured, no precise structure could be deduced.

In the current work, we present a more accurate and unambiguous structure determination of KCN using isotopic substitution. The microwave spectra between 12 and 38 GHz of the ^{13}C and ^{15}N isotopically substituted species of potassium cyanide in the ground vibrational state were measured by molecular beam electric resonance spectroscopy. The seeded-beam technique was used to obtain translational, rotational, and vibrational cooling. For both isotopic species we observed about 20 rotational transitions, which were fitted to an asymmetric rotor model. We determined the rotational, the five quartic, and three sextic distortion constants.

The hyperfine structure of KCN was resolved and identified with the help of microwave–microwave double resonance. One hundred and forty hyperfine transitions in 11 rotational transitions have been assigned. In combination with the results of Törring *et al.* (*8*), we deduced more accurate rotational constants of KCN. The hyperfine spectra of $K^{13}CN$ and $KC^{15}N$ were also unravelled. For all three isotopic species we determined the hyperfine quadrupole coupling constants eQq_{aa} and eQq_{bb} for both potassium and (except for $KC^{15}N$) nitrogen, and some spin–rotation coupling constants.

The rotational constants of all three isotopic species allowed for an unambiguous and accurate structure determination of KCN, which we confirmed to be T shaped. Both the effective structure of the ground vibrational state and the substitution structure were evaluated.

2. EXPERIMENTAL DETAILS

The measurements were performed with the molecular beam electric resonance (MBER) spectrometer described elsewhere (*10, 11*). The experimental conditions are essentially the same as used by Törring *et al.* (*8*). The supply and the nozzle chamber temperatures of the stainless-steel, double-chamber oven were kept at 1150 and 1350 K, respectively. According to Simmons *et al.* (*12*), the supply chamber temperature corresponds to a vapor pressure of monomeric potassium cyanide of about 4 mbar. The stagnation pressure of the carrier gas argon used to produce a seeded beam was 0.6–1 bar. The strong translational, rotational, and vibrational cooling obtained in this way simplified the spectra and enhanced the intensity of the observed transitions considerably by concentrating the population in the low-J states of the ground vi-

brational state. This resulted in a signal-to-noise ratio for the strongest lines of 40 at an integration time of 1 sec. The observed linewidth was about 30 kHz. The frequencies of the observed microwave transitions were determined with an accuracy of typically a few kHz.

An additional advantage of the seeded beam technique (over, e.g., microwave absorption spectroscopy) is a very low material consumption (less than 1 g in 15 hr), which made it possible to study expensive, isotopically enriched samples of $K^{13}CN$ (90%) and $KC^{15}N$ (95%).

3. THEORY

The Hamiltonian used in the fit of the hyperfine spectra of potassium cyanide is (in Cartesian notation) (*13*)

$$H = \sum_{I=1}^{2} [1/6\mathbf{Q}(i) \cdot \mathbf{V}(i)] + \sum_{I=1}^{2} \mathbf{I}_i \cdot \mathbf{M} \cdot \mathbf{J} + \mathbf{I}_1 \cdot \mathbf{D} \cdot \mathbf{I}_2. \tag{1}$$

Herein, $\mathbf{I}_1$ and $\mathbf{I}_2$ are the nuclear spins, $\mathbf{J}$ is the molecular rotational angular momentum; the quantities $\mathbf{Q}$, $\mathbf{V}$, $\mathbf{M}$, and $\mathbf{D}$ are the nuclear quadrupole, electric field gradient, spin–rotation coupling, and spin–spin coupling tensor, respectively. The summation extends over the two nuclei with nonzero spins. The first sum in expression (1) represents the quadrupole interaction, the second sum is the spin–rotation interaction, and the third term describes the spin–spin interaction.

We applied the expressions given by Thaddeus *et al.* (*14*) to obtain the matrix elements of the hyperfine Hamiltonian for the specific case of two interacting nuclei (*11*).

To determine the quadrupole coupling constants eQq_{gg}, the spin–rotation coupling constants M_{gg} and the spin–spin coupling constants D_{gg} with reference to the inertial axes $g = a, b, c$, we constructed a computer program for the hyperfine interaction in molecules with two nuclei possessing couplings of comparable strength, employing the Hamiltonian given by Eq. (1). The following coupling scheme was used:

$$\mathbf{F}_1 = \mathbf{J} + \mathbf{I}_1 \qquad \text{and} \qquad \mathbf{F} = \mathbf{F}_1 + \mathbf{I}_2, \tag{2}$$

where $\mathbf{F}$ is the total angular momentum.

After diagonalization, the energy states are labeled by the quantum numbers J and F, and by a pseudo-spin quantum number ϵ. For a given J and F, the state lowest in energy is denoted with $\epsilon = 1$; the states higher in energy are labeled $\epsilon = 2, 3, \cdots$ consecutively.

The quadrupole and spin–spin coupling constants satisfy Laplace's equation

$$eQq_{aa} + eQq_{bb} + eQq_{cc} = 0, \tag{3}$$

and

$$D_{aa} + D_{bb} + D_{cc} = 0. \tag{4}$$

These constraints are imposed in the calculation. For this reason, eQq_{cc} and D_{cc} are omitted in the list of constants.

4. RESULTS

The analysis of the hyperfine spectrum of the asymmetric rotor molecule potassium cyanide is quite complex because in one rotational transition there are typically about 70 allowed hyperfine transitions (according to the selection rule $\Delta F = 0, \pm 1$) in a frequency region of about 3 MHz. As a consequence of apparatus focusing properties, we only observed a limited number of hyperfine transitions in a given rotational transition.

The problem of identification was solved by the application of microwave–microwave double resonance. This technique was used to analyze the hyperfine spectrum of the a-type (i.e., associated with the electric dipole moment μ_a) $2_{0,2} \rightarrow 1_{0,1}$ and the b-type (i.e., associated with the electric dipole moment μ_b) $1_{1,1} \rightarrow 2_{0,2}$ rotational transition of KCN. A microwave radiation source was scanned around the frequency of the rotational transition while we monitored specific hyperfine components of the $1_{0,1} \rightarrow 0_{0,0}$ and the $2_{0,2} \rightarrow 1_{0,1}$ rotational transitions respectively. In this way a decisive identification was affected. Adding, step by step, more transitions to the least-squares fit for the hyperfine interaction, we were able to assign all observed hyperfine transitions. The same procedure was applied to $K^{13}CN$ and $KC^{15}N$. For these molecules we started with the hyperfine coupling constants ascertained for KCN. By this approach a positive identification was possible without the help of double-resonance spectroscopy. We observed and identified for KCN 140, for $K^{13}CN$ 68, and for $KC^{15}N$ 88 hyperfine transitions in 11, 16, and 20 rotational transitions, respectively (see Appendix).

The best-fit values[3] for the determinable hyperfine coupling constants of KCN, $K^{13}CN$, and $KC^{15}N$ in the ground vibrational state are presented in Table I. The quality of the least-squares fit can be judged[4] from $\sigma = 0.44$, $\sigma = 0.48$, and $\sigma = 0.34$, respectively. The nuclear spin of ^{15}N is ½, so there is no quadrupole interaction due to this nucleus in $KC^{15}N$. For all three isotopic species a reliable determination of the spin–rotation coupling constants of the potassium nucleus and of the spin–rotation coupling constant M_{bb}(N) of the nitrogen nucleus was not possible. These constants were constrained in the fit at zero, as was M_{aa}(N) for $K^{13}CN$ and $KC^{15}N$. The spin–spin coupling constants D_{aa}(K–N) and D_{bb}(K–N) were fixed in the least-squares fit at the values calculated from the effective geometry.

In $K^{13}CN$ all three nuclei possess nonzero spin. The nuclear spin, ½, of ^{13}C gives rise to an additional splitting of the hyperfine transitions due to its spin–rotation and spin–spin interactions. This effect is only marginal, since there was no observable splitting or broadening of the measured hyperfine transitions. This justifies the assumption that the nuclear spin of ^{13}C can be neglected in the fit of the observed hyperfine spectrum.

The hyperfine quadrupole coupling constants are discussed in detail in section 6.

The frequencies ν_0 of the hyperfine-free origins of the rotational transitions are also evaluated in the fit of the hyperfine structure, and are listed in Table II for the three isotope species. These rotational frequencies were fitted by a least-squares method

[3] All uncertainties stated in this paper represent three times the standard deviation as determined by the least-squares fit.

[4] The variance σ is defined as $[\chi^2/(n-m)]^{1/2}$, with χ^2 defined as usual in a least-squares fit, n the number of spectral lines, and m the number of parameters in the fit.

TABLE I

Hyperfine Coupling Constants (*16*) for the Ground Vibrational State of KCN, $K^{13}CN$, and $KC^{15}N$

Constant	KCN	$K^{13}CN$	$KC^{15}N$	Unit
$eQq_{aa}(K)$	-5.605(5)	-5.589(21)	-5.614(8)	MHz
$eQq_{bb}(K)$	2.594(11)	2.594(25)	2.606(7)	MHz
$eQq_{aa}(N)$	1.921(4)	1.909(9)	-	MHz
$eQq_{bb}(N)$	-4.041(15)	-4.019(11)	-	MHz
$M_{aa}(N)$	9.7(6.2)	-	-	kHz
$M_{cc}(N)$	0.70(58)	0.62(50)	1.02(59)	kHz
$D_{aa}(K\text{-}N)$	-0.0454	-0.0450	0.0640	kHz
$D_{bb}(K\text{-}N)$	0.0209	0.0205	-0.0296	kHz

to an asymmetric rotor model based on Watson's reduced Hamiltonian (*15*). The variance σ^4 for the fit of the rotational spectrum of KCN, $K^{13}CN$, and $KC^{15}N$ was 0.36, 0.60, and 0.60, respectively. For KCN, the frequencies given in Table II were combined with the frequencies of the rotational transitions assigned by Törring *et al.* (*8*). The rotational transitions of $K^{13}CN$ and $KC^{15}N$ were identified by the observed hyperfine structure, their optimum voltages for the state selector fields, and their optimum microwave radiation power. For all three isotopic species, we were able to fit the three rotational constants A'', B'', and C'', the five quartic centrifugal distortion constants τ'_{aaaa}, τ'_{bbbb}, τ'_{cccc}, τ_1, and τ_2, as well as three sextic centrifugal distortion constants H_{JK}, H_{KJ}, and h_{JK}. The remaining four sextic distortion constants H_J, H_K, h_J, and h_K were constrained at zero. The results are presented in Table III. The present more accurate results for KCN agree very well with the values obtained by Törring *et al.* (*8*). This is not surprising because preliminary values for the hyperfine-free ν_0 frequencies obtained by Vaals *et al.* (*9*) were already used in their fit.

In the least-squares fit of the rotational spectra the planarity conditions for the τ's were not invoked (*16*). This is a correct approach, since there are five τ's independently determinable and the τ-planarity defect (*16*), $\Delta\tau$, given in Table III, is very large. This indicates that potassium cyanide shows large-amplitude motions.

In Table IV we list the τ-free rotational constants, A, B, and C, and the centrifugal distortion constants τ_{aaaa}, τ_{bbbb}, τ_{aabb}, and τ_{abab}. These molecular parameters were derived assuming planarity (*16*) and using τ_1 and τ_2, or τ_1 and τ'_{cccc}, respectively. The inertial defects $\Delta I = (h/8\pi^2)(1/C - 1/B - 1/A)$ are also listed in Table IV.

The effective moments of inertia I_a, I_b, and I_c in the ground vibrational state were evaluated (*17*) from the τ-free rotational constants using the well-known relations $I_a = h/8\pi^2A$, $I_b = h/8\pi^2B$, and $I_c = h/8\pi^2C$. The results are given in Table IV.

5. STRUCTURE

The structure of a nonsymmetric, nonlinear, triatomic molecule can be derived accurately from the moments of inertia of at least two isotopic species. So, we are now in the position to remove the ambiguity in the structure derived by Törring *et*

TABLE II

Frequencies (in MHz) of the Observed[a] and Calculated Hyperfine-Free Origins of the Rotational Transitions of KCN, $K^{13}CN$, and $KC^{15}N$ in the Ground Vibrational State

Isotope	J'	K_{-1}'	K_1'	J''	K_{-1}''	K_1''	Type	Obs. frequency	Obs.-calc.
KCN	1	0	1	0	0	0	a	9475.4865(30)	0.0045
	2	0	2	1	0	1	a	18948.5547(30)	0.0018
	3	0	3	2	0	2	a	28416.8015(20)	-0.0009
	4	0	4	3	0	3	a	37877.8223(20)	-0.0007
	8	1	7	8	1	8	a	14529.2077(70)	0.0017
	9	1	8	9	1	9	a	18157.1001(80)	-0.0032
	4	2	3	3	2	2	a	37886.9672(80)	0.0047
	1	1	1	2	0	2	b	34375.9059(30)	0.0007
	2	1	2	3	0	3	b	24504.6206(30)	0.0006
	3	1	3	4	0	4	b	14443.3633(30)	-0.0008
	7	0	7	6	1	6	b	16795.7519(70)	-0.0008
$K^{13}CN$	2	0	2	1	0	1	a	18465.8935(90)	0.0018
	4	0	4	3	0	3	a	36912.2301(40)	0.0003
	8	1	7	8	1	8	a	14343.9584(70)	0.0032
	9	1	8	9	1	9	a	17925.3794(60)	-0.0018
	19	2	17	19	2	18	a	13059.473(20)	-0.0148
	20	2	18	20	2	19	a	15781.880(20)	0.0196
	21	2	19	21	2	20	a	18864.081(20)	-0.0057
	1	1	1	2	0	2	b	32700.0794(90)	-0.0028
	3	1	3	4	0	4	b	13263.7935(70)	-0.0006
	7	0	7	6	1	6	b	17208.5231(60)	-0.0009
	11	2	10	12	1	11	b	27986.980(18)	0.0029
	12	2	11	13	1	12	b	16268.537(19)	-0.0034
	17	1	16	16	2	15	b	32244.202(20)	0.0004
	21	3	19	22	2	20	b	36812.959(20)	0.0010
	23	3	21	24	2	22	b	12520.298(20)	-0.0017
	26	2	24	25	3	23	b	12824.249(20)	-0.0007
$KC^{15}N$	2	0	2	1	0	1	a	18564.6047(40)	0.0018
	3	0	3	2	0	2	a	27840.7939(40)	0.0009
	4	0	4	3	0	3	a	37109.6539(30)	0.0010
	8	1	7	8	1	8	a	14409.3837(60)	-0.0002
	9	1	8	9	1	9	a	18007.3133(80)	0.0031
	11	1	10	11	1	11	a	26391.7895(80)	0.0057
	12	1	11	12	1	12	a	31174.6757(80)	-0.0003
	13	1	12	13	1	13	a	36348.0219(80)	-0.0045
	19	2	17	19	2	18	a	13099.9462(40)	-0.0029
	20	2	18	20	2	19	a	15832.1421(40)	0.0008
	21	2	19	21	2	20	a	18925.9161(40)	0.0013
	23	2	21	23	2	22	a	26260.1079(40)	0.0006
	24	2	22	24	2	23	a	30524.6567(40)	-0.0012
	1	1	1	2	0	2	b	32939.0431(30)	-0.0017
	7	0	7	6	1	6	b	17235.2403(40)	-0.0031
	11	2	10	12	1	11	b	28330.3342(70)	0.0003
	12	2	11	13	1	12	b	16548.3697(70)	0.0012
	17	1	16	16	2	15	b	32230.0446(90)	0.0021
	21	3	19	22	2	20	b	37305.990(16)	0.0004
	26	2	24	25	3	23	b	12615.525(10)	-0.0028

[a]The observed frequencies (16) are evaluated in the least-squares fit of the observed hyperfine spectrum.

al. (*8*). We fitted I_a, I_b, and I_c of KCN, $K^{13}CN$, and $KC^{15}N$ to determine the effective structure of potassium cyanide in the ground vibrational state. The result is presented in Table V, and corresponds to "structure B" of Törring *et al.* (*8*).

All possible combinations of pairs of moments of inertia of two isotopic species yield structural parameters well within the uncertainties given in Table V. Only when I_a is left out is there a significant deviation of the structural parameters of up to 0.03 Å for the CN bond length. This is caused by the fortuity that $|a_i| \simeq r_i \equiv (a_i^2 + b_i^2)^{1/2}$ for all three nuclei, especially for potassium, where $|a_i| - r_i \simeq 0.00007$ Å. We define a_i and b_i as the coordinates of the nucleus i in the principal axes system. Since $I_b = \Sigma_i m_i a_i^2$ and $I_c = \Sigma_i m_i r_i^2$, the calculated structure is inaccurate if $I_a = \Sigma_i m_i b_i^2$ is excluded from the fit. The small inconsistency of structures calculated

TABLE III

Rotational Constants (*16*) for the Ground Vibrational State of KCN, $K^{13}CN$, and $KC^{15}N$

Constant	KCN	$K^{13}CN$	$KC^{15}N$	Unit
A"	58265.8452(35)	55984.083(15)	56347.208(6)	MHz
B"	4940.0540(4)	4816.796(3)	4842.403(2)	MHz
C"	4536.2176(5)	4418.098(4)	4441.900(3)	MHz
τ_{aaaa}'	-5.360(12)	-5.28(7)	-4.65(6)	MHz
τ_{bbbb}'	-0.02699(2)	-0.0266(2)	-0.0254(2)	MHz
τ_{cccc}'	-0.01882(4)	-0.0184(3)	-0.0178(2)	MHz
τ_1	-1.55628(63)	-1.4294(68)	-1.5369(61)	MHz
τ_2	-0.12089(6)	-0.1131(7)	-0.1198(6)	MHz
H_{JK}	-4.71(14)	-4.3(4)	-4.18(7)	Hz
H_{KJ}	95(3)	96(19)	89(8)	Hz
h_{JK}	-2.4(2.1)	-7.5(3.0)	-3.6(8)	Hz
$\Delta\tau$	-0.95(2)	-0.89(6)	-0.88(2)	kHz

from different combinations of I's and different pairs of isotopic species is a consequence of zero-point vibrations, as illustrated by the finite τ-planarity and inertial defect.

The substitution structure, given in Table V, is obtained using Kraitchman's equations (*18*). For the location of the carbon and the nitrogen nuclei we applied these equations on the observed isotope shifts in the moments of inertia of the ^{13}C and ^{15}N isotopically substituted molecular species. Since we did not observe the spectrum of the ^{41}KCN molecule, the coordinates of the potassium nucleus were determined by invoking the first-moment (i.e. center of mass) condition (*19*). It is favorable to determine the position of the potassium nucleus in this way because it is located very close to a principal axis (b_K = 0.012 Å). In such cases Kraitchman's equations cannot be used for accurate coordinate calculations. However, the error in the position is independent of the coordinate value, when the first-moment condition is used.

The uncertainties in the substitution structural parameters are estimated from the value of the inertial defect and from comparison with other molecules (*20*). It was shown by Costain (*21*) that the zero-point vibrational effects tend to cancel in the calculation of the substitution structure, which is expected (*21, 22*) to be closer to the equilibrium structure than the effective structure.

The values of the structural parameters r_{KC} and r_{KN} are larger for the effective than for the substitution structure. This can be understood from the same considerations as used for the bond length in a diatomic molecule (*20*) with stretch vibration (K–[CN]). The value of r_{CN}, however, decreases. This can be explained from the large bending vibration, which can be considered as a wagging of the C–N axis. The stretch vibrations can be neglected, and the value of the effective bond length is the result

TABLE IV

Derived Molecular Constants for the Ground Vibrational State of KCN, $K^{13}CN$, and $KC^{15}N$

Constant	KCN	$K^{13}CN$	$KC^{15}N$	Unit
From τ_1 and τ_2, assuming planarity:				
A	58265.3905	55983.660	56346.771	MHz
B	4939.6565	4816.430	4842.012	MHz
C	4536.0698	4417.967	4441.747	MHz
τ_{aaaa}	-5.360	-5.28	-4.65	MHz
τ_{bbbb}	-0.02699	-0.0266	-0.0254	MHz
τ_{aabb}	0.14827	0.1499	0.1198	MHz
τ_{abab}	-0.88762	-0.8255	-0.8540	MHz
ΔI	0.4291	0.4364	0.4365	amuÅ^2
From τ_1 and τ_{cccc}', assuming planarity:				
A	58265.4330	55983.699	56346.809	MHz
B	4939.6602	4816.434	4842.015	MHz
C	4536.0450	4417.944	4441.724	MHz
τ_{aaaa}	-5.360	-5.28	-4.65	MHz
τ_{bbbb}	-0.02699	-0.0266	-0.0254	MHz
τ_{aabb}	0.05575	0.0650	0.0363	MHz
τ_{abab}	-0.80206	-0.7471	-0.7769	MHz
ΔI	0.4298	0.4371	0.4372	amuÅ^2
From the τ-free rotational constants:				
I_a	8.67374(5)	9.02726(5)	8.96908(5)	amuÅ^2
I_b	102.3105(30)	104.9281(30)	104.3737(30)	amuÅ^2
I_c	111.4137(30)	114.3920(30)	113.7796(30)	amuÅ^2

for the "effective" projection of the vibrating C and N nuclei on the equilibrium position of the C–N axis.

6. DISCUSSION

The measurements of Törring *et al.* (*8*) and the preliminary results of the current work (*9*) showed that the structure of potassium cyanide is T shaped. This unusual structure stimulated *ab initio* calculations of the potential energy surface for both potassium (*1, 2*) and sodium cyanide (*2*), as well as for lithium isocyanide (*3, 23*). We established experimentally that the structure of NaCN is also T shaped (*24*), and that LiNC has a linear isocyanide structure (*10*).

In Table VI are listed some results of *ab initio* calculations on KCN. The quantities E(KCN) and E(KNC) are defined as the energies of the linear cyanide and isocyanide

TABLE V

Effective Structural Parameters (*16*) for the Ground Vibrational State and Substitution Structural Parameters (in Å) for Potassium Cyanide

	r_{CN}	r_{KC}	r_{KN}
effective structure	1.169(3)	2.716(9)	2.549(9)
substitution structure	1.174(2)	2.711(5)	2.532(5)

configurations, respectively, relative to the energy of the T-shaped configuration. Although there is an explicit discrepancy for the various theoretical predictions of *E*(KCN) and *E*(KNC), the agreement between the calculated results for the structure and the accurate experimental values is gratifying.

The hyperfine quadrupole coupling constants given in Table VI are obtained[5] from the *ab initio* field gradients by a transformation of the calculated quadrupole coupling matrices to the principal inertia axes system of the *ab initio* structures. In brackets, we have shown the results for a transformation to the principal inertia axes system of the experimental effective structure. A comparison of the listed values for the quadrupole coupling constants with the experimental results given in Table I shows that the constants, with respect to the experimental structure, are in better agreement that the values with respect to the *ab initio* structure. The agreement is very good for the field gradients calculated by Wormer *et al.* (*1*), if transformed to the experimental structure.

[5] We employed $Q(^{39}K) = 0.059$ barn, and $Q(^{14}N) = 0.0166$ barn. These values are from C. M. Lederer, and V. S. Shirley (eds.), "Table of Isotopes," 7th ed., Wiley, New York, 1978.

TABLE VI

Summary of Results of *ab initio* Calculations on KCN (The hyperfine coupling constants (*28*) are given for the *ab initio* structure, and in brackets for the experimental structure (see text).)

Constant	Wormer *et al.* (2)	Klein *et al.* (3)	Marsden (3)	Unit
E(KCN)	2020	2280	1090	cm^{-1}
E(KNC)	494	600	1170	cm^{-1}
r_{CN}	1.157	1.153	1.14	Å
r_{KC}	2.906	2.850	2.80	Å
r_{KN}	2.582	2.616	2.65	Å
$eQq_{aa}(K)$	-5.582(-5.670)	-4.638(-4.940)	–	MHz
$eQq_{bb}(K)$	2.633(2.721)	1.753(2.055)	–	MHz
$eQq_{aa}(N)$	1.513(1.913)	1.758(1.896)	–	MHz
$eQq_{bb}(N)$	-3.458(-3.858)	-3.758(-3.896)	–	MHz

TABLE VII

Principal Hyperfine Quadrupole Coupling Constants for Potassium Cyanide in the Ground Vibrational State

Constant	Potassium	Nitrogen	Unit
eQq_x	2.637(9)	1.995(23)	MHz
eQq_z	-5.645(10)	-4.110(25)	MHz
η	0.066(4)	0.029(13)	
$\theta(a,z)$	-4.0(7)	83.7(1.0)	degree
$\theta(z,C\text{-}N)$	85.9(7)	-1.8(1.0)	degree

Since we determined the quadrupole coupling constants eQq_{aa} and eQq_{bb} in more than one isotopic species, the principal elements eQq_x(K), eQq_z(K) and eQq_x(N), eQq_z(N) of the quadrupole coupling tensors for potassium and nitrogen can be evaluated (*25*). The results are presented in Table VII, including the asymmetry parameter $\eta = (eQq_x - eQq_y)/eQq_z$. In Fig. 1 is shown the orientation of the principal inertial (a, b, c) and quadrupole (x, y, z) axes. The y axis coincides with the c axis. The z axis is chosen as the axis for which the coupling of the nucleus approximately has axial symmetry. In Table VII are also listed the angles between the z axis of the principal quadrupole system for potassium and nitrogen, z_K and z_N, respectively, and the principal inertial axis a and the C–N axis, respectively.

As a consequence of the almost completely ionic bonding,[6] and the large distance of the potassium nucleus to the CN group, we expect that the CN group can be considered as a free CN^- ion. This picture is supported by the following arguments. The determined asymmetry parameters η indicate that the couplings are practically axially symmetric ($eQq_x \simeq eQq_y \simeq -\frac{1}{2}eQq_z$). For nitrogen, the z axis almost coincides with the C–N axis. So, the coupling at the nitrogen nucleus is approximately symmetric about the bond axis between the carbon and the nitrogen. Furthermore, the value for eQq_z(N) is close to the quadrupole coupling constant eQq(N) = −4.090 MHz evaluated[5] from the field gradient for the free CN^- ion obtained by Wormer (*26*) in a SCF calculation using 54 contracted Gaussian-type orbitals at r_{CN} = 1.174 Å. Finally, we expect the equilibrium CN bond length in KCN to be close to the equilibrium value (*27*) of r_{CN} = 1.173(2) Å in the CN^- ion. There is, indeed, a very good correspondence between this value and the substitution bond length r_{CN} = 1.174(2) Å given in Table V.

Ab initio calculations (*28, 29*) of the rovibrational spectrum of KCN suffer from serious inaccuracies when the *ab initio* potential is used. If, however, the *ab initio* potential energy is shifted to the experimental geometry (*28*), the difference between the theoretical and observed spectrum diminishes dramatically. From the inertial

[6] This can be inferred from *ab initio* calculations (Refs. (*2, 3*)) and is confirmed by preliminary results for the electric dipole moments μ_a = 11(1) D and μ_b = 6(2) D, which we obtained from measurements in nonzero electric fields using the molecular beam electric resonance technique.

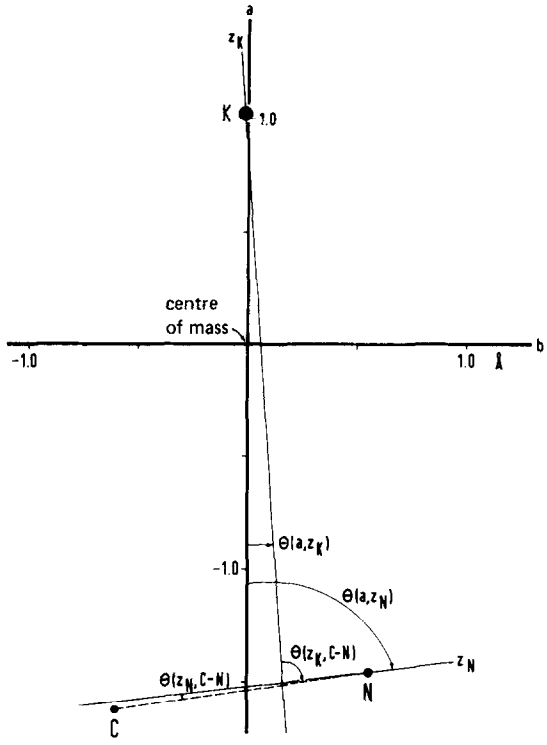

FIG. 1. Orientation of the principal axes of inertia (a, b, c) and the principal axes of the field gradient (x, y, z) in the potassium cyanide molecule. The c and y axes coincide and are perpendicular to the molecular plane. The subscripts K and N are added to clarify the distinction between the potassium and the nitrogen quadrupole principal axes.

defects ΔI, listed in Table IV, we can estimate (*20*) the bending vibrational frequencies $\omega_2 \simeq h/2\pi^2\Delta I$. These are 157(30), 154(30), and 154(30) cm^{-1} for KCN, $K^{13}CN$, and $KC^{15}N$, respectively. This is in gratifying agreement with the results from matrix-isolation studies (*5*) (139 cm^{-1}) and *ab initio* calculations (*28, 29*) (116–120 cm^{-1}), but in disagreement with the frequency, ω_2 = 207(20) cm^{-1}, obtained by Leroi and Klemperer (*30*) from infrared absorption studies. Tennyson and Sutcliffe (*28*) suggested that the observed absorption corresponds to a bending overtone. This is not very probable, since it can be deduced from intensity considerations that the symmetric stretching mode, ω_1, should also have been observed by Leroi and Klemperer (*30*), which was not the case. The interpretation of Ismail *et al.* (*5*), that the spectrum of KOCN, and not KCN, is observed in the infrared absorption cell seems more likely.

An effort to evaluate the quadratic force constants from the quartic distortion constants determined from the rotational spectrum was unsuccessful. Even the inclusion of the inertial defect and the vibrational frequencies from matrix-isolation studies (*5*) did not yield a stable solution. This is a consequence of the large anharmonicity of the potential energy surface (*1, 2, 28, 29*).

The discrepancies in the thermodynamic data for potassium cyanide (*5, 12, 31*) from mass spectrometric studies and calculations based on the second and third law,

can be explained by analogous arguments. In all calculations an incorect structure, usually linear, of KCN was assumed. However, by moderate thermal excitation the K^+ cation can tunnel through the low bending potential barriers, or even orbit around the CN^- anion. Consequently, for a range of temperatures no specific structure or vibrational frequencies can be assigned.

The rotational spectrum of KCN in the ground vibrational state can still properly be described by the semirigid rotor model. The low bending vibrational frequency, ω_2, however, indicates that the molecule is very floppy. Since the potential energy barriers in the bending directions, E(KCN) and E(KNC), are low, only a few excitations of the bending vibration will change the effective structure and increase the bending vibrational amplitude considerably. The bonding then becomes more and more "polytopic," and a new description of the rotation–vibration spectrum (*28, 29, 32*) is necessary. An experimental investigation of KCN, NaCN, and LiNC in vibrational excited states is planned in our laboratory. Hopefully, this will yield detailed information on thc rovibrational spectrum and will give a decisive result for the values of E(KCN) and E(KCN), now disputed (see Table VI) by various *ab initio* calculations.

APPENDIX

Frequencies (in MHz) of the observed and calculated hyperfine transitions of KCN in the ground vibrational state. Transitions measured using the microwave-microwave double resonance technique are marked •. The corresponding hyperfine components monitored to observe the double resonance spectrum are marked ¤.

$F_\varepsilon' \rightarrow F_\varepsilon''$	Obs. frequency	Obs.-calc.	$F_\varepsilon' \rightarrow F_\varepsilon''$	Obs. frequency	Obs.-calc
Rotational transition $1_{0,1} \rightarrow 0_{0,0}$:			$9/2_1 \rightarrow 7/2_2$	28414.9398(30)	0.0025
$7/2_1 \rightarrow 5/2_1$	9475.6680(60)	-0.0031	$7/2_1 \rightarrow 7/2_2$	28415.2151(60)	-0.0034
$5/2_2 \rightarrow 5/2_1$	9476.1140(60)¤	-0.0015	$9/2_1 \rightarrow 9/2_1$	28415.4859(80)	0.0024
$1/2_2 \rightarrow 1/2_1$	9476.9100(30)¤	0.0008	$5/2_1 \rightarrow 3/2_2$	28415.4859(80)	0.0016
$3/2_3 \rightarrow 3/2_1$	9477.0510(30)¤	0.0003	$7/2_1 \rightarrow 5/2_3$	28415.6728(80)	0.0014
Rotational transition $2_{0,2} \rightarrow 1_{0,1}$:			$7/2_2 \rightarrow 7/2_2$	28415.6728(80)	-0.0001
$3/2_3 \rightarrow 3/2_3$	18948.4376(60)•	-0.0016	$7/2_1 \rightarrow 9/2_1$	28415.7663(60)	0.0016
$1/2_2 \rightarrow 3/2_3$	18948.5350(60)•	-0.0020	$3/2_1 \rightarrow 5/2_3$	28415.8940(60)	-0.0047
$3/2_3 \rightarrow 1/2_2$	18948.5795(60)•	-0.0013	$1/2_1 \rightarrow 1/2_2$	28416.0023(40)	-0.0005
$1/2_2 \rightarrow 1/2_2$	18948.6781(60)•	-0.0004	$1/2_1 \rightarrow 3/2_3$	28416.0986(40)	-0.0019
$7/2_2 \rightarrow 5/2_2$	18948.7321(80)•	-0.0055	$3/2_1 \rightarrow 3/2_2$	28416.1778(40)	0.0019
$5/2_1 \rightarrow 3/2_1$	18949.176(10)	-0.0046	$5/2_3 \rightarrow 3/2_3$	28416.4406(50)	-0.0004
$7/2_2 \rightarrow 7/2_1$	18949.176(10)	-0.0061	$3/2_2 \rightarrow 1/2_2$	28416.7313(60)	-0.0002
$5/2_2 \rightarrow 5/2_1$	18949.512(12)	-0.0038	$7/2_3 \rightarrow 9/2_1$	28416.8134(60)	0.0001
$3/2_2 \rightarrow 5/2_1$	18949.7210(90)¤	-0.0010	$9/2_1 \rightarrow 7/2_1$	28416.8254(60)	0.0030
$3/2_3 \rightarrow 3/2_2$	18949.9902(60)	0.0036	$3/2_2 \rightarrow 3/2_3$	28416.8299(80)	0.0006
$3/2_2 \rightarrow 3/2_1$	18950.2345(90)	0.0006	$5/2_1 \rightarrow 3/2_1$	28416.8299(80)	-0.0024
$5/2_3 \rightarrow 3/2_1$	18950.5099(90)	-0.0012	$9/2_2 \rightarrow 7/2_2$	28416.8835(80)	-0.0023
$1/2_2 \rightarrow 1/2_1$	18950.8601(30)¤	0.0007	$5/2_2 \rightarrow 5/2_2$	28416.9143(60)	-0.0024
$3/2_3 \rightarrow 5/2_1$	18951.0903(30)¤	0.0013	$7/2_2 \rightarrow 7/2_1$	28417.5618(80)	0.0038
$3/2_3 \rightarrow 3/2_1$	18951.6037(90)	0.0028	$5/2_2 \rightarrow 5/2_1$	28417.7681(60)	0.0039
$1/2_2 \rightarrow 3/2_1$	18951.7006(90)	0.0020	$5/2_2 \rightarrow 7/2_1$	28417.8593(30)	-0.0065
Rotational transition $3_{0,3} \rightarrow 2_{0,2}$:			$5/2_2 \rightarrow 3/2_1$	28418.0634(80)	0.0046
$3/2_1 \rightarrow 1/2_2$	28414.7135(30)	0.0023	$7/2_3 \rightarrow 7/2_1$	28418.1529(80)	0.0007
$5/2_1 \rightarrow 7/2_2$	28414.7557(30)	0.0015	$9/2_2 \rightarrow 7/2_1$	28418.7759(60)	0.0049
$3/2_1 \rightarrow 3/2_3$	28414.8070(30)	-0.0019	$1/2_1 \rightarrow 3/2_1$	28418.8164(60)	0.0009

APPENDIX—*Continued*

$F_\varepsilon' \rightarrow F_\varepsilon''$	Obs. frequency	Obs.-calc.	$F_\varepsilon' \rightarrow F_\varepsilon''$	Obs. frequency	Obs.-calc.
$5/2_3 \rightarrow 5/2_1$	28418.8603(80)	-0.0011	$21/2_2 \rightarrow 21/2_1$	18159.5175(80)	-0.0005
$5/2_3 \rightarrow 7/2_1$	28418.9640(60)	0.0010	$21/2_2 \rightarrow 19/2_1$	18159.9819(80)	-0.0009
Rotational transition $4_{0,4} \rightarrow 3_{0,3}$:			Rotational transition $4_{2,3} \rightarrow 3_{2,2}$:		
$3/2_1 \rightarrow 3/2_2$	37877.0211(80)	-0.0006	$7/2_3 \rightarrow 9/2_2$	37877.3342(80)	0.0058
$9/2_3 \rightarrow 9/2_2$	37877.2157(80)	0.0024	$5/2_2 \rightarrow 7/2_2$	37877.5307(80)	-0.0058
$7/2_1 \rightarrow 7/2_1$	37877.416(10)	0.0064	Rotational transition $1_{1,1} \rightarrow 2_{0,2}$:		
$3/2_1 \rightarrow 5/2_3$	37877.416(10)	0.0056	$3/2_1 \rightarrow 1/2_2$	34372.9843(30)•	-0.0013
$7/2_3 \rightarrow 5/2_3$	37877.6512(50)	0.0005	$3/2_1 \rightarrow 3/2_3$	34373.0840(40)•	0.0007
$5/2_2 \rightarrow 3/2_2$	37877.7484(80)	0.0020	$1/2_1 \rightarrow 1/2_2$	34373.4004(50)•	-0.0015
$3/2_1 \rightarrow 1/2_1$	37877.7484(80)	-0.0021	$5/2_1 \rightarrow 3/2_3$	34373.4515(70)•	0.0023
$7/2_3 \rightarrow 9/2_2$	37877.8389(80)	-0.0039	$1/2_1 \rightarrow 3/2_3$	34373.5004(50)•	0.0008
$11/2_1 \rightarrow 9/2_1$	37877.8389(80)	-0.0031	$5/2_1 \rightarrow 7/2_2$	34374.0842(30)	-0.0019
$11/2_2 \rightarrow 9/2_2$	37877.8640(30)	-0.0023	$3/2_1 \rightarrow 5/2_3$	34374.1732(50)	0.0001
$5/2_2 \rightarrow 5/2_3$	37878.1360(30)	0.0013	$3/2_1 \rightarrow 3/2_2$	34374.4509(70)•	0.0006
$11/2_2 \rightarrow 11/2_1$	37878.4507(50)	0.0015	$1/2_2 \rightarrow 3/2_3$	34374.4792(60)•	0.0024
$3/2_1 \rightarrow 5/2_2$	37878.503(12)	-0.0041	$3/2_2 \rightarrow 1/2_2$	34374.5771(70)•	0.0025
$7/2_2 \rightarrow 7/2_1$	37878.5335(50)	-0.0000	$3/2_2 \rightarrow 3/2_3$	34374.6758(50)•	0.0035
$7/2_3 \rightarrow 5/2_2$	37878.746(12)	-0.0016	$5/2_1 \rightarrow 3/2_2$	34374.8183(70)•	0.0021
$7/2_2 \rightarrow 9/2_1$	37878.817(12)	0.0022	$5/2_2 \rightarrow 3/2_3$	34375.0498(60)•	0.0037
$7/2_3 \rightarrow 7/2_2$	37879.0526(80)	-0.0032	$7/2_1 \rightarrow 7/2_2$	34375.1716(30)	-0.0000
$9/2_3 \rightarrow 9/2_1$	37879.1620(60)	0.0001	$5/2_2 \rightarrow 7/2_2$	34375.6808(30)	-0.0022
$5/2_2 \rightarrow 5/2_2$	37879.2327(60)	0.0008	$3/2_2 \rightarrow 5/2_3$	34375.7643(40)	0.0022
$3/2_1 \rightarrow 5/2_1$	37879.7351(80)	0.0014	$5/2_2 \rightarrow 5/2_3$	34376.1362(50)	0.0003
$5/2_2 \rightarrow 3/2_1$	37879.765(12)	-0.0021	$5/2_2 \rightarrow 3/2_2$	34376.412(10)	-0.0009
$7/2_3 \rightarrow 9/2_1$	37879.7921(50)	0.0008	$5/2_2 \rightarrow 5/2_2$	34376.6185(70)	-0.0006
Rotational transition $8_{1,7} \rightarrow 8_{1,8}$:			Rotational transition $2_{1,2} \rightarrow 3_{0,3}$:		
$21/2_1 \rightarrow 19/2_1$	14529.921(10)	-0.0008	$5/2_1 \rightarrow 5/2_3$	24502.6374(40)	0.0008
$17/2_2 \rightarrow 17/2_1$	14530.0875(80)	0.0002	$3/2_1 \rightarrow 5/2_3$	24502.8006(50)	-0.0020
$17/2_3 \rightarrow 19/2_1$	14530.4140(80)	-0.0021	$7/2_1 \rightarrow 5/2_3$	24502.9079(40)	-0.0011
$17/2_3 \rightarrow 15/2_1$	14530.6402(80)	0.0021	$7/2_1 \rightarrow 9/2_2$	24503.1015(30)	0.0005
$17/2_3 \rightarrow 17/2_1$	14530.871(10)	0.0005	$5/2_1 \rightarrow 7/2_3$	24503.4479(70)	0.0005
Rotational transition $9_{1,8} \rightarrow 9_{1,9}$:			$7/2_2 \rightarrow 9/2_2$	24503.6488(30)	0.0000
$19/2_2 \rightarrow 17/2_1$	18157.816(15)	0.0074	$5/2_1 \rightarrow 5/2_2$	24503.7345(50)	0.0007
$19/2_3 \rightarrow 21/2_1$	18158.291(10)	0.0037	$3/2_1 \rightarrow 5/2_2$	24503.9011(50)	0.0013
$17/2_3 \rightarrow 19/2_1$	18158.966(12)	-0.0069	$9/2_1 \rightarrow 9/2_2$	24504.0913(80)	-0.0038

APPENDIX—*Continued*

$F_\varepsilon' \rightarrow F_\varepsilon''$	Obs. frequency	Obs.-calc.	$F_\varepsilon' \rightarrow F_\varepsilon''$	Obs. frequency	Obs.-calc.
$7/2_2 \rightarrow 7/2_3$	24504.270(10)	0.0025	$5/2_3 \rightarrow 5/2_2$	14442.9362(80)	0.0003
$5/2_1 \rightarrow 3/2_1$	24504.270(10)	0.0015	$7/2_1 \rightarrow 9/2_1$	14443.0087(80)	0.0021
$5/2_2 \rightarrow 7/2_3$	24504.4024(70)	-0.0015	$9/2_1 \rightarrow 9/2_2$	14443.0899(80)	-0.0004
Rotational transition $3_{1,3} \rightarrow 4_{0,4}$:			$5/2_2 \rightarrow 7/2_2$	14443.2030(80)	-0.0005
$5/2_1 \rightarrow 5/2_2$	14441.1875(80)	-0.0006	$5/2_3 \rightarrow 7/2_3$	14443.421(10)	0.0006
$5/2_1 \rightarrow 7/2_3$	14441.672(10)	-0.0003	$3/2_2 \rightarrow 3/2_1$	14443.421(10)	0.0039
$9/2_1 \rightarrow 11/2_2$	14441.7443(60)	-0.0039	$11/2_1 \rightarrow 13/2_1$	14443.5249(80)	-0.0008
$3/2_1 \rightarrow 5/2_2$	14441.8081(60)	0.0017	$7/2_2 \rightarrow 9/2_2$	14443.6438(80)	-0.0013
$5/2_1 \rightarrow 3/2_1$	14441.9136(60)	0.0008	$9/2_1 \rightarrow 11/2_1$	14443.7192(80)	-0.0018
$7/2_1 \rightarrow 9/2_3$	14442.0169(60)	0.0021	Rotational transition $7_{0,7} \rightarrow 6_{1,6}$:		
$7/2_2 \rightarrow 7/2_3$	14442.3243(60)	-0.0021	$15/2_1 \rightarrow 13/2_1$	16796.1599(70)	0.0028
$7/2_1 \rightarrow 7/2_2$	14442.3649(80)	0.0030	$11/2_2 \rightarrow 9/2_2$	16796.440(10)	0.0004
$9/2_2 \rightarrow 11/2_2$	14442.4577(60)	-0.0009	$15/2_2 \rightarrow 13/2_1$	16796.440(10)	-0.0042
$5/2_1 \rightarrow 7/2_2$	14442.6520(60)	0.0034	$17/2_2 \rightarrow 15/2_2$	16796.4972(90)	-0.0015
$7/2_1 \rightarrow 9/2_2$	14442.7013(60)	-0.0027			

Frequencies (in MHz) of the observed and calculated hyperfine transitions of $K^{13}CN$ in the ground vibrational state.

$F_\varepsilon' \rightarrow F_\varepsilon''$	Obs. frequency	Obs.-calc.	$F_\varepsilon' \rightarrow F_\varepsilon''$	Obs. frequency	Obs.-calc.
Rotational transition $2_{0,2} \rightarrow 1_{0,1}$:			$9/2_3 \rightarrow 9/2_2$	36911.6259(60)	0.0004
$3/2_2 \rightarrow 3/2_1$	18467.5640(80)	-0.0014	$7/2_3 \rightarrow 5/2_3$	36912.0581(80)	-0.0012
$5/2_3 \rightarrow 3/2_1$	18467.8374(80)	-0.0041	$5/2_2 \rightarrow 3/2_2$	36912.1550(60)	0.0010
$1/2_2 \rightarrow 1/2_1$	18468.1926(60)	0.0007	$11/2_2 \rightarrow 9/2_2$	36912.2704(80)	-0.0032
$3/2_3 \rightarrow 5/2_1$	18468.4213(40)	0.0011	$5/2_2 \rightarrow 5/2_3$	36912.5420(80)	0.0023
Rotational transition $4_{0,4} \rightarrow 3_{0,3}$:			$5/2_1 \rightarrow 5/2_1$	36912.7995(80)	0.0072
$3/2_1 \rightarrow 3/2_2$	36911.4342(60)	-0.0010	$7/2_3 \rightarrow 7/2_2$	36913.4567(60)	-0.0033

APPENDIX—*Continued*

$F_\varepsilon' \rightarrow F_\varepsilon''$	Obs. frequency	Obs.-calc.
Rotational transition $8_{1,7} \rightarrow 8_{1,8}$:		
$11/2_1 \rightarrow 13/2_1$	14344.3906(80)	-0.0030
$17/2_2 \rightarrow 19/2_1$	14344.3906(80)	0.0037
$21/2_1 \rightarrow 19/2_1$	14344.6690(80)	-0.0031
$17/2_2 \rightarrow 17/2_1$	14344.833(10)	-0.0055
$15/2_3 \rightarrow 17/2_2$	14345.151(10)	0.0027
$17/2_3 \rightarrow 15/2_1$	14345.388(12)	0.0084
$17/2_3 \rightarrow 17/2_1$	14345.6115(70)	0.0003
Rotational transition $9_{1,8} \rightarrow 9_{1,9}$:		
$19/2_1 \rightarrow 19/2_1$	17925.4546(90)	0.0010
$19/2_2 \rightarrow 19/2_2$	17925.6094(80)	0.0022
$19/2_2 \rightarrow 17/2_2$	17925.7786(90)	0.0042
$13/2_1 \rightarrow 15/2_1$	17925.8398(90)	-0.0023
$19/2_2 \rightarrow 21/2_1$	17925.8398(90)	0.0015
$17/2_2 \rightarrow 19/2_2$	17925.980(10)	-0.0066
$19/2_2 \rightarrow 17/2_1$	17926.0918(80)	0.0030
$23/2_1 \rightarrow 21/2_1$	17926.0918(80)	0.0011
$17/2_2 \rightarrow 17/2_2$	17926.158(10)	0.0035
$17/2_3 \rightarrow 19/2_2$	17926.554(10)	0.0048
$19/2_3 \rightarrow 21/2_1$	17926.554(10)	-0.0054
$17/2_3 \rightarrow 19/2_1$	17927.2366(80)	-0.0057
$15/2_2 \rightarrow 15/2_1$	17927.7334(90)	0.0053
$21/2_2 \rightarrow 21/2_1$	17927.7838(90)	-0.0036
$21/2_2 \rightarrow 19/2_1$	17928.2482(60)	-0.0016
Rotational transition $19_{2,17} \rightarrow 19_{2,18}$:		
$43/2_1 \rightarrow 43/2_1$	13059.228(20)	0.0049
$35/2_2 \rightarrow 35/2_2$	13059.955(20)	-0.0049
Rotational transition $20_{2,18} \rightarrow 20_{2,19}$:		
$45/2_1 \rightarrow 45/2_1$	15781.603(20)	-0.0056
$43/2_2 \rightarrow 43/2_2$	15782.416(20)	0.0056
Rotational transition $21_{2,19} \rightarrow 21_{2,20}$:		
$43/2_1 \rightarrow 43/2_1$	18863.825(20)	0.0041
$43/2_3 \rightarrow 43/2_2$	18864.724(20)	-0.0041
Rotational transition $1_{1,1} \rightarrow 2_{0,2}$:		
$3/2_1 \rightarrow 1/2_2$	32697.1706(80)	-0.0032
$3/2_1 \rightarrow 3/2_3$	32697.2775(80)	0.0067
$5/2_1 \rightarrow 7/2_2$	32698.2708(80)	-0.0024
$3/2_1 \rightarrow 5/2_3$	32698.3566(80)	-0.0012
Rotational transition $3_{1,3} \rightarrow 4_{0,4}$:		
$5/2_1 \rightarrow 5/2_2$	13261.6273(70)	-0.0015
$3/2_1 \rightarrow 5/2_2$	13262.2442(60)	-0.0011
$5/2_1 \rightarrow 3/2_1$	13262.3422(60)	-0.0054
$7/2_1 \rightarrow 9/2_3$	13262.4516(70)	0.0012
$7/2_2 \rightarrow 7/2_3$	13262.7626(70)	0.0055
$7/2_1 \rightarrow 7/2_2$	13262.8026(70)	0.0037
Rotational transition $7_{0,7} \rightarrow 6_{1,6}$:		
$15/2_1 \rightarrow 13/2_1$	17208.9254(60)	-0.0014
$11/2_2 \rightarrow 9/2_2$	17209.2094(80)	0.0031
$15/2_2 \rightarrow 13/2_1$	17209.2094(80)	-0.0001
$17/2_2 \rightarrow 15/2_2$	17209.2644(60)	-0.0003
Rotational transition $11_{2,10} \rightarrow 12_{1,11}$:		
$23/2_2 \rightarrow 25/2_3$	27986.170(20)	-0.0098
$23/2_2 \rightarrow 25/2_2$	27986.796(30)	0.0142
$21/2_3 \rightarrow 23/2_2$	27987.373(20)	0.0035
Rotational transition $12_{2,11} \rightarrow 13_{1,12}$:		
$27/2_1 \rightarrow 27/2_2$	16267.747(20)	0.0049
$27/2_2 \rightarrow 29/2_2$	16267.747(20)	-0.0104
$23/2_3 \rightarrow 25/2_2$	16268.937(30)	0.0124
Rotational transition $17_{1,16} \rightarrow 16_{2,15}$:		
$33/2_2 \rightarrow 31/2_3$	32243.819(20)	-0.0053
$37/2_2 \rightarrow 35/2_2$	32244.932(20)	0.0053
Rotational transition $21_{3,19} \rightarrow 22_{2,20}$:		
$45/2_2 \rightarrow 47/2_2$	36812.477(20)	-0.0082
$37/2_1 \rightarrow 39/2_1$	36813.202(20)	0.0082
Rotational transition $23_{3,21} \rightarrow 24_{2,22}$:		
$49/2_2 \rightarrow 51/2_2$	12519.786(20)	0.0007
$45/2_3 \rightarrow 47/2_2$	12520.565(20)	-0.0007
Rotational transition $26_{2,24} \rightarrow 25_{3,23}$:		
$51/2_2 \rightarrow 49/2_3$	12823.963(20)	-0.0035
$55/2_2 \rightarrow 53/2_2$	12824.798(20)	0.0035

APPENDIX—*Continued*

Frequencies (in MHz) of the observed and calculated hyperfine transitions of $KC^{15}N$ in the ground vibrational state.

$F_\varepsilon' \rightarrow F_\varepsilon''$	Obs. frequency	Obs.-calc.
Rotational transition $2_{0,2} \rightarrow 1_{0,1}$:		
$2_2 \rightarrow 2_2$	18564.3294(70)	0.0048
$2_1 \rightarrow 2_1$	18564.717(15)	-0.0072
$3_2 \rightarrow 3_1$	18564.717(15)	-0.0074
$1_1 \rightarrow 1_1$	18565.728(12)	0.0006
$1_2 \rightarrow 1_1$	18567.1311(50)	-0.0009
Rotational transition $3_{0,3} \rightarrow 2_{0,2}$:		
$4_1 \rightarrow 4_1$	27839.4499(80)	-0.0067
$1_1 \rightarrow 1_2$	27840.5122(50)	0.0000
$3_1 \rightarrow 3_1$	27840.8628(80)	0.0037
$4_2 \rightarrow 4_1$	27840.8628(80)	0.0033
$2_1 \rightarrow 2_1$	27841.5152(70)	-0.0003
Rotational transition $4_{0,4} \rightarrow 3_{0,3}$:		
$3_1 \rightarrow 3_2$	37109.5313(40)	-0.0002
$2_1 \rightarrow 2_2$	37109.5313(40)	-0.0008
$4_1 \rightarrow 4_1$	37109.6955(50)	0.0014
$5_2 \rightarrow 5_1$	37109.6955(50)	0.0007
$3_1 \rightarrow 3_1$	37110.1883(60)	-0.0001
$2_1 \rightarrow 2_1$	37110.9368(80)	-0.0013
Rotational transition $8_{1,7} \rightarrow 8_{1,8}$:		
$6_1 \rightarrow 6_1$	14409.335(15)	0.0095
$10_1 \rightarrow 10_1$	14409.335(15)	-0.0042
$7_1 \rightarrow 7_1$	14409.433(15)	0.0065
$9_1 \rightarrow 9_1$	14409.433(15)	-0.0073
$8_2 \rightarrow 8_1$	14409.6767(90)	-0.0017
Rotational transition $9_{1,8} \rightarrow 9_{1,9}$:		
$7_1 \rightarrow 7_1$	18007.261(15)	0.0040
$11_1 \rightarrow 11_1$	18007.261(15)	-0.0073
$8_1 \rightarrow 8_1$	18007.365(15)	0.0073
$10_1 \rightarrow 10_1$	18007.365(15)	-0.0040
Rotational transition $11_{1,10} \rightarrow 11_{1,11}$:		
$9_1 \rightarrow 9_1$	26391.738(15)	0.0034
$13_1 \rightarrow 13_1$	26391.738(15)	-0.0040
$10_1 \rightarrow 10_1$	26391.840(15)	0.0040
$12_1 \rightarrow 12_1$	26391.840(15)	-0.0034
Rotational transition $12_{1,11} \rightarrow 12_{1,12}$:		
$10_1 \rightarrow 10_1$	31174.623(15)	0.0005
$14_1 \rightarrow 14_1$	31174.623(15)	-0.0053
$11_1 \rightarrow 11_1$	31174.728(15)	0.0053
$13_1 \rightarrow 13_1$	31174.728(15)	-0.0006
Rotational transition $13_{1,12} \rightarrow 13_{1,13}$:		
$11_1 \rightarrow 11_1$	36347.969(15)	-0.0005
$15_1 \rightarrow 15_1$	36347.969(15)	-0.0049
$12_1 \rightarrow 12_1$	36348.075(15)	0.0049
$14_1 \rightarrow 14_1$	36348.075(15)	0.0005
Rotational transition $19_{2,17} \rightarrow 19_{2,18}$:		
$17_1 \rightarrow 17_1$	13099.9300(80)	-0.0014
$21_1 \rightarrow 21_1$	13099.9300(80)	-0.0005
$18_1 \rightarrow 18_1$	13099.9624(80)	0.0005
$20_1 \rightarrow 20_1$	13099.9624(80)	0.0014
Rotational transition $20_{2,18} \rightarrow 20_{2,19}$:		
$18_1 \rightarrow 18_1$	15832.1274(80)	0.0012
$22_1 \rightarrow 22_1$	15832.1274(80)	0.0025
$19_1 \rightarrow 19_1$	15832.1568(80)	-0.0025
$21_1 \rightarrow 21_1$	15832.1568(80)	-0.0012
Rotational transition $21_{2,19} \rightarrow 21_{2,20}$:		
$19_1 \rightarrow 19_1$	18925.8979(80)	-0.0012
$23_1 \rightarrow 23_1$	18925.8979(80)	0.0005
$20_1 \rightarrow 20_1$	18925.9343(80)	-0.0005
$22_1 \rightarrow 22_1$	18925.9343(80)	0.0012
Rotational transition $23_{2,21} \rightarrow 23_{2,22}$:		
$21_1 \rightarrow 21_1$	26260.0877(80)	-0.0012
$25_1 \rightarrow 25_1$	26260.0877(80)	0.0014
$22_1 \rightarrow 22_1$	26260.1280(80)	-0.0014

APPENDIX—*Continued*

$F_\varepsilon' \rightarrow F_\varepsilon''$	Obs. frequency	Obs.-calc.	$F_\varepsilon' \rightarrow F_\varepsilon''$	Obs. frequency	Obs.-calc.
$24_1 \rightarrow 24_1$	26260.1280(80)	0.0012	$12_1 \rightarrow 12_1$	28330.364(12)	0.0024
Rotational transition $24_{2,22} \rightarrow 24_{2,23}$:			$11_2 \rightarrow 11_1$	28330.364(12)	-0.0049
$22_1 \rightarrow 22_1$	30524.6369(80)	0.0001	Rotational transition $12_{2,11} \rightarrow 13_{1,12}$:		
$26_1 \rightarrow 26_1$	30524.6369(80)	0.0032	$14_1 \rightarrow 14_2$	16548.359(12)	0.0058
$23_1 \rightarrow 23_1$	30524.6765(80)	-0.0032	$11_2 \rightarrow 11_1$	16548.359(12)	-0.0019
$25_1 \rightarrow 25_1$	30524.6765(80)	-0.0001	$13_1 \rightarrow 13_1$	16548.392(12)	0.0019
Rotational transition $1_{1,1} \rightarrow 2_{0,2}$:			$12_2 \rightarrow 12_1$	16548.392(12)	-0.0058
$0_1 \rightarrow 0_1$	32936.9888(40)	0.0000	Rotational transition $17_{1,16} \rightarrow 16_{2,15}$:		
$1_2 \rightarrow 1_2$	32938.1603(60)	0.0005	$16_1 \rightarrow 16_2$	32230.037(15)	0.0042
$3_1 \rightarrow 3_2$	32938.5115(40)	-0.0011	$15_1 \rightarrow 15_2$	32230.037(15)	0.0028
$2_2 \rightarrow 2_2$	32939.5648(50)	0.0008	$17_1 \rightarrow 17_1$	32230.037(15)	-0.0028
$2_2 \rightarrow 2_1$	32940.5680(40)	0.0003	$18_2 \rightarrow 18_1$	32230.037(15)	-0.0042
Rotational transition $7_{0,7} \rightarrow 6_{1,6}$:			Rotational transition $21_{3,19} \rightarrow 22_{2,20}$:		
$6_1 \rightarrow 6_2$	17235.1880(70)	0.0012	$23_1 \rightarrow 23_2$	37305.999(30)	0.0122
$7_1 \rightarrow 7_1$	17235.2213(70)	0.0011	$20_2 \rightarrow 20_1$	37305.999(30)	0.0094
$5_1 \rightarrow 5_2$	17235.2382(70)	-0.0024	$22_1 \rightarrow 22_1$	37305.999(30)	-0.0095
$8_2 \rightarrow 8_1$	17235.2746(70)	0.0005	$21_2 \rightarrow 21_1$	37305.999(30)	-0.0122
$6_1 \rightarrow 6_1$	17235.5144(80)	0.0027	Rotational transition $26_{2,24} \rightarrow 25_{3,23}$:		
$5_1 \rightarrow 5_1$	17236.5975(70)	-0.0024	$25_1 \rightarrow 25_2$	12615.515(15)	0.0023
Rotational transition $11_{2,10} \rightarrow 12_{1,11}$:			$24_1 \rightarrow 24_2$	12615.515(15)	0.0006
$13_1 \rightarrow 13_2$	28330.315(12)	0.0049	$26_1 \rightarrow 26_1$	12615.515(15)	-0.0006
$10_2 \rightarrow 10_1$	28330.315(12)	-0.0025	$27_2 \rightarrow 27_1$	12615.515(15)	-0.0023

ACKNOWLEDGMENTS

The authors wish to express their gratitude to Dr. P. E. S. Wormer for calculating the field gradient at the nitrogen nucleus in the CN^- ion and kindly allowing us to publish his result. They thank Dr. J. P. Bekooy for his continuing interest and the many helpful discussions that we have enjoyed with him. This work is part of the research program of the Stichting voor Fundamenteel Onderzoek der Materie (F.O.M.) and has been made possible by financial support from the Nederlandse Organisatie voor Zuiver Wetenschappelijk Onderzoek (Z.W.O.).

RECEIVED: December 22, 1983

REFERENCES

1. P. E. S. WORMER AND J. TENNYSON, *J. Chem. Phys.* **75**, 1245–1252 (1981).
2. M. L. KLEIN, J. D. GODDARD, AND D. G. BOUNDS, *J. Chem. Phys.* **75**, 3909–3915 (1981); C. J. MARSDEN, *J. Chem. Phys.* **76**, 6451–6452 (1982).
3. R. ESSERS, J. TENNYSON, AND P. E. S. WORMER, *Chem. Phys. Lett.* **89**, 223–227 (1982).

4. E. CLEMENTI, H. KISTENMACHER, AND H. POPKIE, *J. Chem. Phys.* **58,** 2460–2466 (1973).
5. Z. K. ISMAIL, R. H. HAUGE, AND J. L. MARGRAVE, *J. Mol. Spectrosc.* **45,** 304–315 (1973).
6. W. J. PIETRO, B. A. LEVI, W. J. HEHRE, AND R. F. STEWART, *Inorg. Chem.* **19,** 2225–2229 (1980).
7. P. KUIJPERS, T. TÖRRING, AND A. DYMANUS, *Chem. Phys. Lett.* **42,** 423–428 (1976).
8. T. TÖRRING, J. P. BEKOOY, W. L. MEERTS, J. HOEFT, E. TIEMANN, AND A. DYMANUS, *J. Chem. Phys.* **73,** 4875–4882 (1980).
9. J. J. VAN VAALS, W. L. MEERTS, AND A. DYMANUS, *in* "34th Symposium on Molecular Spectroscopy," Columbus, Ohio, 1980; "7th Colloquium on High Resolution Spectroscopy," Reading, 1981.
10. J. J. VAN VAALS, W. L. MEERTS, AND A. DYMANUS, *Chem. Phys.* **82,** 385–393 (1983).
11. J. J. VAN VAALS, Ph.D. Thesis, Katholieke Universiteit Nijmegen, The Netherlands, 1983.
12. L. L. SIMMONS, L. F. LOWDEN, AND T. C. EHLERT, *J. Phys. Chem.* **81,** 709–712 (1977).
13. J. VERHOEVEN, AND A. DYMANUS, *J. Chem. Phys.* **52,** 3222–3233 (1970).
14. P. THADDEUS, L. C. KRISHER, AND J. H. N. LOUBSER, *J. Chem. Phys.* **40,** 257–273 (1964).
15. J. K. G. WATSON, *J. Chem. Phys.* **46,** 1935–1949 (1967); *J. Chem. Phys.* **48,** 4517–4524 (1968).
16. W. H. KIRCHHOFF, *J. Mol. Spectrosc.* **41,** 333–380 (1972).
17. E. R. COHEN, AND B. N. TAYLOR, *J. Phys. Chem. Ref. Data* **2,** 663–734 (1973).
18. J. KRAITCHMAN, *Amer. J. Phys.* **21,** 17–24 (1953).
19. D. R. LIDE, JR., *in* "Molecular Structure and Properties" (A. D. Buckingham, ed.) Vol. 2, Butterworths, London, 1975.
20. W. GORDY AND R. L. COOK, "Microwave Molecular Spectra," Interscience, New York, 1970.
21. C. C. COSTAIN, *J. Chem. Phys.* **29,** 864–874 (1958).
22. J. K. G. WATSON, *J. Mol. Spectrosc.* **48,** 479–502 (1973).
23. C. J. MARSDEN, private communication.
24. J. J. VAN VAALS, W. L. MEERTS, AND A. DYMANUS, *J. Chem. Phys.* **77,** 5245–5246 (1982).
25. D. W. POSENER, *Austr. J. Phys.* **13,** 168–185 (1960).
26. P. E. S. WORMER, private communication.
27. P. R. TAYLOR, G. B. BACSKAY, N. S. HUSH, AND A. C. HURLEY, *J. Chem. Phys.* **70,** 4481–4490 (1979).
28. J. TENNYSON AND B. T. SUTCLIFFE, *Mol. Phys.* **46,** 97–109 (1982).
29. J. TENNYSON AND A. VAN DER AVOIRD, *J. Chem. Phys.* **76,** 5710–5718 (1982); J. TENNYSON AND B. T. SUTCLIFFE, *J. Chem. Phys.* **77,** 4061–4072 (1982).
30. G. E. LEROI AND W. KLEMPERER, *J. Chem. Phys.* **35,** 774–775 (1961).
31. JANAF, "Thermochemical Tables," 2nd ed., U. S. Department of Commerce, National Bureau of Standards, Washington, D. C., 1971; J. N. MULVIHILL AND L. F. PHILLIPS, *Chem. Phys. Lett.* **33,** 608–611 (1975); B. V. L'VOV AND L. A. PELIEVA, *Prog. Anal. Atom. Spectrosc.* **3,** 65–86 (1980); K. SKUDLARSKI AND M. MILLER, *Advan. Mass. Spectrom.* **8,** 433–444 (1980); *High Temp. Sci.* **15,** 151–163 (1982).
32. V. A. ISTOMIN, N. F. STEPANOV, AND B. I. ZHILINSKII, *J. Mol. Spectrosc.* **67,** 265–282 (1977); B. I. ZHILINSKII, V. A. ISTOMIN, AND N. F. STEPANOV, *Chem. Phys.* **31,** 413–423 (1978); P. R. BUNKER AND D. J. HOWE, *J. Mol. Spectrosc.* **83,** 288–303 (1980); G. BROCKS AND J. TENNYSON, *J. Mol. Spectrosc.* **99,** 263–278 (1983); O. S. VAN ROOSMALEN, F. IACHELLO, R. D. LEVINE, AND A. E. L. DIEPERINK, preprint.